

Importance of the RpoE Regulon in Maintaining the Lipid Bilayer during Antimicrobial Treatment with the Polycationic Agent, Chlorhexidine

Sinisa Vidovic, Prabhakara Medihala, James J. Dynes, Prasad Daida, Vladimir Vujanovic, Adam P. Hitchcock, Deeksha Shetty, Haixia Zhang, David R. Brown, John R. Lawrence, and Darren R. Korber*

The emergence of multidrug resistance in bacteria has reached alarming levels. To solve this growing problem, discovery of novel cellular targets or pathways important for antimicrobial resistance is urgently needed. In this study, we explored how the alternative sigma factor, RpoE, protects *Escherichia coli* O157 against the toxic effects of the polycationic antimicrobial agent, chlorhexidine (CHX). Susceptibility of this organism to CHX was found to directly correlate to the growth rate, with the faster replicating wild-type being more susceptible to CHX than its more slowly replicating $\Delta rpoE$ O157 mutant. Once the wild-type and *rpoE* mutant strains had undergone growth arrest (entered the stationary growth phase), their resistance to CHX became entirely dependent on the functionality of RpoE. The RpoE regulon plays a critical role in maintaining the integrity of the asymmetric lipid bilayer of *E. coli*, thereby preventing the intracellular accumulation of CHX. Finally, using a single-cell, high-resolution, synchrotron-based approach, we discovered a subpopulation of the *rpoE* mutant strain with no detectable intracellular CHX, a predominant characteristic of the wild-type CHX-resistant population. This finding reveals a role of phenotypic heterogeneity in antimicrobial resistance.

the CDC,^[2] Gram-negative pathogens pose the most significant threat, as they are the predominant cause of mortality among patients infected with multidrug resistant bacteria. Higher rates of mortality caused by Gram-negative bacteria can be explained by their profound intrinsic antimicrobial resistance. Gram-negative bacteria possess a unique structural feature, the outer membrane, which confers intrinsic antimicrobial resistance to this group of prokaryotes. The alternative sigma factor, RpoE (σ^E), is a regulatory protein that plays a crucial role in the response to various stressors that affect the synthesis, assembly, and homeostasis of lipopolysaccharides (LPS) and outer-membrane porins (OMPs), essential structures of outer membrane in Gram-negative bacteria.^[3] These responses are generally known as extracytoplasmic stress responses (ESRs). The stressors that activate ESRs include a wide range of stimuli, including both abiotic (e.g., heat shock,^[4] cold shock,^[5] oxidative stress,^[6] exposure to zinc nanoparticles,^[7] and detergents^[8]) and biotic (e.g., biofilm formation^[9] as well as growth in vivo^[10]) stimuli. In

1. Introduction

The emergence of multidrug resistant bacteria has become a growing threat to public health worldwide.^[1,2] According to

Prof. Dr. S. Vidovic, Prof. Dr. D. R. Brown
Department of Veterinary and Biomedical Sciences
College of Veterinary Medicine
University of Minnesota
Saint Paul, MN, USA

Dr. P. Medihala, Dr. P. Daida, Prof. Dr. V. Vujanovic, D. Shetty, Dr. D. R. Korber
Department of Food and Bioproduct Sciences
University of Saskatchewan
Saskatoon, Canada
E-mail: darren.korber@usask.ca

Dr. J. J. Dynes
Canadian Light Source, Inc.
University of Saskatchewan
Saskatoon, Canada

Prof. Dr. A. P. Hitchcock
Brockhouse Institute for Materials Research
McMaster University
Hamilton, Canada

Dr. H. Zhang
Department of Plant Sciences
University of Saskatchewan
Saskatoon, Canada

Dr. J. R. Lawrence
Environment Canada
Saskatoon, Canada

DOI: 10.1002/pmic.201700285

Significance of the study

The emergence of multidrug resistance has become one of the most concerning public health problems worldwide. To solve this growing problem, discovery of novel cellular targets or pathways involved in intrinsic or acquired antimicrobial resistance is urgently needed. In this study, we explored how the alternative sigma factor, RpoE (σ^E), protects enterohemorrhagic *Escherichia coli* against the polycationic antimicrobial agent, chlorhexidine (CHX), during the exponential and stationary growth phases. We found that the *rpoE* mutation conferred growth phase-dependent changes in tolerance to CHX. In the exponential growth phase, the *rpoE* mutant, inherently growth deficient (i.e., slow replicating), showed reduced susceptibility to CHX compared to the wild type. Upon entry into the stationary growth-phase, which is characterized by growth arrest, the wild type exhibited resistance, whereas the *rpoE* mutant showed a significant susceptibility. Using scanning transmission X-ray microscopy to examine individual cells, we found that the integrity of the lipid bilayer became compromised, leading to intracellular accumulation of CHX in the *rpoE* mutant and development of a predominantly “leaky-cell” phenotype. Our data showed that the σ^E regulon plays a critical role in the homeostasis of *E. coli* exposed to polycationic agents by maintaining the integrity of the lipid bilayer of the outer membrane.

Gram-negative bacteria, the activation of the σ^E stress-response system is initiated by the presence of misfolded proteins in the periplasm,^[8] as well as off-pathway intermediates in LPS transport and assembly.^[11] These dual-molecular signals activate regulated intra-membrane proteolysis,^[12] a conserved signal transduction pathway that results in the release of cytoplasmic membrane-bound σ^E . Once released, σ^E binds to the core RNA polymerase and initiates transcription of a group of genes that are widely conserved across Gram-negative bacteria along with a set of more variable genes.^[13] The synthesis of the σ^E -conserved gene products results in the activation of periplasmic chaperones, trans-envelope complexes, proteases and other regulators that are involved in biogenesis of the asymmetric lipid bilayer of outer membrane and OMPs.^[11,13]

2. Experimental Section

2.1. Bacterial Strains, Growth Conditions, and Antimicrobial Agents

Escherichia coli K-12 strain DH5 α was used as the host for the recombinant plasmids pSV8, pSV9, and pSV190, while *E. coli* SM10 λ pir strain was used to maintain the recombinant plasmid pSV10. The wild-type *E. coli* O157 strain B-1 was previously described.^[14] Plasmids pUC19, pRE112, pACYC184, and pTrc99A were used as cloning vectors. Growth media were supplemented with chloramphenicol (30 $\mu\text{g mL}^{-1}$), ampicillin (100 $\mu\text{g mL}^{-1}$), nalidixic acid (50 $\mu\text{g mL}^{-1}$), or tetracycline (15 $\mu\text{g mL}^{-1}$) (Sigma Chemical Co., St. Louis, MO) for

maintenance of recombinant plasmids and selection of the bacterial strains, as required.

2.2. Construction of $\delta rpoE$ *E. coli* O157 Mutant and Complementation Study

Creation of an *rpoE* in-frame deletion mutant of *E. coli* O157 was carried out as described elsewhere.^[15] Two DNA fragments, each containing a small *rpoE* terminal coding sequence (either 5' or 3') and the 950-bp region that flanks the *rpoE* gene, were amplified using chromosomal DNA of *E. coli* O157 B-1. The specific primers for the upstream fragment were RPOE F1 5'-CCC GGT ACC GTA GTA AGG AGA AAG GCG TTT GAA ATC GGT-3' and RPOE R1 5'-CCC GAG CTC GAG CGA GGG AAG CTA TTG ATA ACA AAG TTC-3'. The downstream fragment was amplified using primers RPOE F2 5'-GGG GAG CTC CCC TTC TGG ACC CGT TCA ACC AGG ACC TGG-3' and RPOE R2 5'-GTG GAG CCC GGG CAC CGC CGG TTG CCA GCA CCA CCG CTT TTG-3'. Sucrose-resistant and chloramphenicol-sensitive transconjugants represented the second recombination event where 84% of the wild-type *rpoE* gene of *E. coli* O157 B-1 was deleted, resulting in strain SV-522. The deletion of the *rpoE* gene in strain SV-522 was confirmed by both PCR analysis and DNA sequencing. Plasmids pTrc99A-*rpoE* and pTrc99A (courtesy of Carol Gross and Susan Gottesman) were used to complement the *E. coli* O157 SV-522 (e.g., *rpoE* mutant) and *E. coli* O157 B-1 (e.g., wild type) strains, respectively. An intact *rpoE* gene was cloned under the *lacI* promoter of pTrc99A. A gene complementation study was then carried out as described next.

2.3. Extracytoplasmic Stress Assay

Stress assays were performed using overnight cultures of the wild-type *E. coli* O157 B-1 and its $\Delta rpoE$ SV-522 *E. coli* O157 mutant that had been grown in LB at 37 °C with constant shaking at 190 rpm. These seed cultures were diluted 1/100 in 100 mL of freshly prepared LB and grown at 37 °C to optical densities at 600 nm of 0.4 and 1. These mid-exponential and early stationary growth phase cultures were immediately exposed to chlorhexidine (CHX) at a final concentration of 10 $\mu\text{g mL}^{-1}$. CHX challenge was maintained in suspension with shaking at 190 rpm and incubated for additional 3 h. Viable cell counts were performed by tenfold serial dilutions in 0.9% NaCl at time zero (before CHX exposure) and then at every 30 min of the incubation. Aliquots of 0.1 mL were plated on LB agar in triplicate and then incubated at 37°C for 24 h.

In addition, to rule out any effect of the stationary growth phase on the survivability of the *rpoE* mutant, both untreated wild-type and *rpoE* mutant strains were grown to an OD₆₀₀ of 1, and enumerated in triplicate on LB plates over a 3-h incubation period, as described above.

2.4. Sample Preparation for Protein Analysis

Cultures (10 mL volume) of the wild-type *E. coli* O157 B-1 and $\Delta rpoE$ mutant *E. coli* O157 SV-522 strains previously exposed to

CHX for 0 (before exposure), 30, and 60 min were centrifuged at $13\,680 \times g$ for 5 min. The resultant cell pellets were washed twice in sterile water and frozen at -70°C .

2.5. 2D-DIGE Analysis

2.5.1. Protein Labeling and 2D Electrophoresis

Total cellular protein was extracted from resuspended cell pellets in 1 mL of lysis buffer (GE Healthcare Bio-Science, Inc., Baie d'Urfe, Quebec, Canada). The cell lysis solution was then centrifuged at $13\,680 \times g$ for 5 min. The resulting supernatant was resuspended in the equal volume of ice-cold acetone thrice and then incubated overnight at -20°C to precipitate the proteins. The precipitated proteins were isolated by centrifugation at $13\,680 \times g$ for 15 min and then solubilized in cell lysis buffer containing 7 M urea, 2 M thiourea, 4% (w/v) CHAPS, and 30 mM Tris-Cl. Total protein was quantified using a 2D Quant kit (GE Healthcare, Mississauga, ON). The protein solution was cleaned up using a 2D Cleanup kit according to the manufacturer's instructions (GE Healthcare). Proteins were labeled using fluorescent cyanine dyes according to the manufacturer's instructions (GE Healthcare). Cyanine dyes were freshly reconstituted in dimethylformamide and added to the labeling reactions at a ratio of 400 pmol dye to 50 μg protein. Labeling reactions were incubated in the dark for 30 min on ice, after which the reactions were terminated by the addition of 10 mM lysine (1 μL per 400 pmol dye). Each replicate within the group was labeled with either Cy3 or Cy5 or both. The pooled internal standard was labeled with Cy2 fluorescent dye. Isoelectric focusing and SDS-PAGE were performed using Ready Strip IPGv (Bio-Rad) and 14% [w/v] sodium dodecyl sulfate-polyacrylamide gels.

2.5.2. Gel Image Analysis

Analysis of scanned images was carried out using ImageQuant V5.0 and DeCyder Version 7.0 2D software (GE Healthcare), according to the manufacturer's recommendations. Gel spots were first detected with background subtraction and then a DIGE approach was used with an internal standard to perform accurate matching between samples and generate a ratio of protein abundance for each protein of interest. As the internal standard was included in each gel, this allowed normalization of all the data. During the second analysis step, the biological variation method was used to match multiple images from different gels and to provide statistical analyses for quantitative comparisons of spot volumes between all the samples. Statistically significant differences between protein spots were attained when they contained at least 1.5-fold changes and $p < 0.05$.

2.5.3. LC-MS/MS and Protein Identification

Protein spot excision for protein identification was carried out using the robotic Ettan Spot Picker (GE Healthcare) system. For each protein spot, gel slices were excised and treated with 10 mM dithiothreitol (DTT) for 30 min at 37°C , followed by alkylation, achieved by adding 50 μL of 55 mM iodoacetamide for 20 min also at 37°C . Proteins were digested in-gel using

buffer supplemented with 0.01 $\mu\text{g} \mu\text{L}^{-1}$ trypsin (Promega, Madison, WI) in 20 nM ammonium bicarbonate. After overnight incubation at 37°C , peptides were extracted three times by sonication in solvent containing 50% (v/v) acetonitrile with 0.1% (v/v) TFA. Elutes were collected and completely dried by vacuum centrifugation. Peptides were then desalted using a C18 column (Waters, Milford, MA), reconstituted in 40 μL of 0.1% formic acid and 3% acetonitrile, and analyzed in a nano-flow ultraperformance LC (nano-Acquity, Waters) unit coupled with an ESI Q-TOF Ultima (Waters) tandem mass spectrometer. The data were analyzed using MassLynx ver. 4.0 software and processed by the ProteinLynx global server (version 2.2; Waters). The obtained peak patterns were searched against the NCBI database using the MASCOT (Matrix Science Ltd., London, UK) search engine.

2.6. Validation of Proteomic Data by Real-Time PCR

Synthesis of cDNA was carried out using iScriptTM Reverse Transcription (Bio-Rad Laboratories, Inc. Hercules, CA). q-PCR was performed on a MiniOpticonTM Real-Time PCR Detection System (Bio-Rad Laboratories) with iQTM SYBR[®] Green Supermix kit (Bio-Rad Laboratories). Gene *gyrA*, encoding for DNA gyrase, type II topoisomerase, was selected as an internal reference gene. The expression of *gyrA* in the wild-type and $\Delta rpoE$ mutant was not affected by growth phase, CHX treatment, or *rpoE* mutation. Primers were designed to target expression of the following genes: *ompA*, *fumC*, *IpdA*, *ycsC*, and *tuf*. Data were analyzed according to methods described previously.^[16]

2.7. Scanning Transmission X-Ray Microscopy (STXM) and Data Analysis

Samples were measured using STXM on the SM (10ID1) beamline at the Canadian Light Source Synchrotron (CLS, Saskatoon, Canada).^[17] Image sequences were collected at the C K-edge (280–320 eV) and the measured transmitted signal (*I*) was converted to absorbance ($A = -\ln(I/I_0)$) using the incident flux (*I*₀) measured through regions of the dry cell devoid of bacteria. The singular value decomposition procedure was used to derive quantitative (i.e., thickness in nm) component maps of the major biomacromolecules using suitable reference spectra—proteins (human serum albumin), lipids (1,2-dipalmitoyl-*sn*-glycerol-3-phosphocholine), and polysaccharides (xanthan gum), as well as $(\text{CO}_3)^2$ (CaCO_3)², K^+ (K_2CO_3) with the $(\text{CO}_3)^2$ derived from calcium carbonate subtracted, and CHX. The spectrum at each pixel in the image sequence was fit to the spectra of the reference compounds that had been placed on an absolute linear absorbance scale.^[18] The reliability and methodology used to quantitatively map the major biomacromolecules and CHX in cells have been described in detail elsewhere.^[19] Curve fitting of spectra extracted from the component maps using grayscale threshold masking was also performed as a check on the reliability of the component maps. All reference compounds were from Sigma-Aldrich, except human serum albumin (Behringwerke AG), and were of a minimum purity of 98%. The C K-edge energy scale of the microscope was calibrated using the Rydberg peak (294.96 eV) of CO_2 .

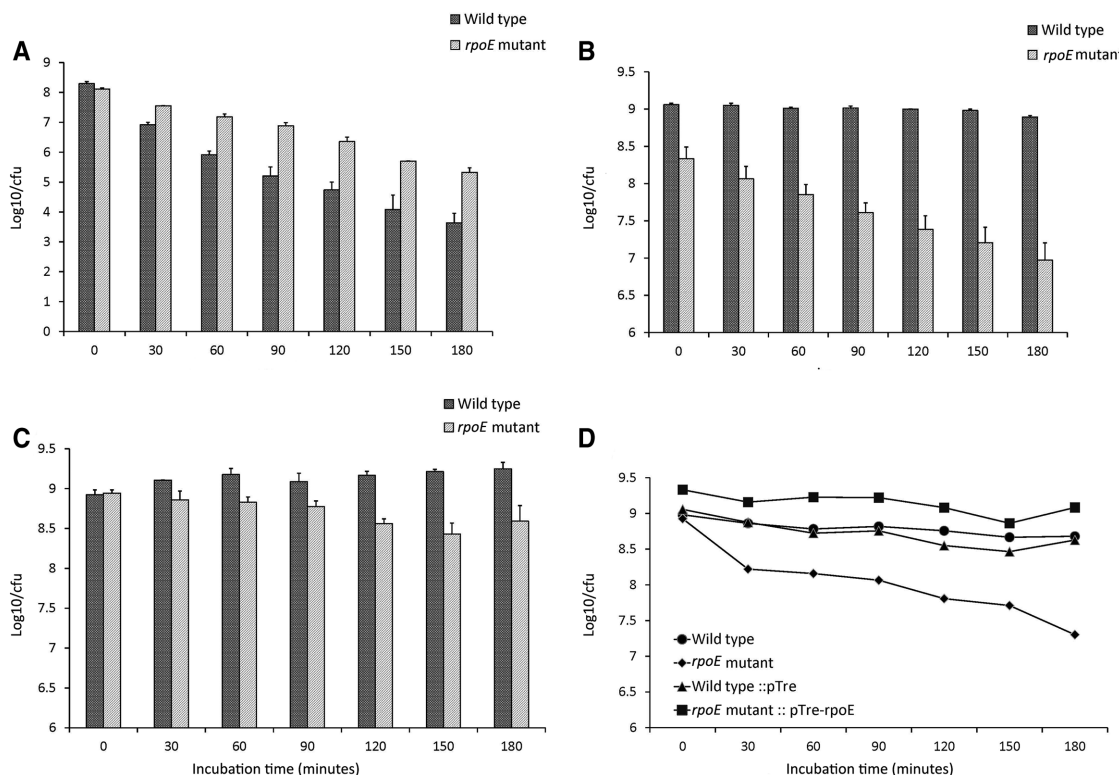


Figure 1. Evaluation of the effect of CHX on the wild-type *Escherichia coli* O157 and the $\Delta rpoE$ mutant strains during (A) exponential and (B) stationary growth phases. Validation of the effect of the stationary growth phase on the survivability of untreated *rpoE* mutant cells (C). The effect of the dysfunctional *rpoE* gene on cell survival during CHX treatment, as well as the survival of respective gene-complemented strains (D).

2.8. Experimental Replication and Bioinformatics

Data from the extracytoplasmic stress assays represent the average of three biological replicates, while data from proteomics and transcriptomics represent the average of two biological replicates. Kinetic data were analyzed by CoStat version 6.4 software (CoHort Software, Monterey, CA) using the homogeneity of linear regression slopes method to test for significant ($p < 0.05$) differences. Analyses of variance were used to reveal statistically significant differences in protein abundance. The correlation test between the proteomic (DIGE) data and the transcriptomic (q-PCR) data was done using the linear regression model implemented in R.^[20] The gene ontology (GO) analysis was conducted using the Database for Annotation, Visualization and Integrated Discovery (DAVID) database.^[21]

3. Results

3.1. Growth Phase-Dependent CHX Inhibition

The homogeneity of linear regression slope analysis revealed a statistically significant ($p < 0.05$) bactericidal effect of CHX on both organisms during exponential growth phase (Figure 1A). However, the death rate for wild-type *E. coli* O157 was significantly ($p = 0.0025$) higher than that of the *rpoE* mutant. Intriguingly, during the early stationary growth phase, CHX did not impose any lethal effect on wild-type *E. coli* O157, resulting in

no mortality rate for this organism; whereas, the *rpoE* mutant experienced a substantial decline in the number of viable cells (Figure 1B) during the same treatment. Analysis of the survival curve slopes revealed a significant difference ($p = 0.0000$) between the survival of the wild-type strain and its *rpoE* mutant (Figure 1B). To rule out any effect of the stationary growth phase on the mortality rate of the *rpoE* mutant, we carried out another assay. Our data showed that the stationary phase had a minor effect on the mortality rate of untreated *rpoE* mutant cells (Figure 1C). Comparison of the decline (e.g., 0.35-fold) caused by the stationary growth phase with the decline of the *rpoE* mutant caused by the CHX treatment (e.g., 1.36-fold) resulted in a statistically significant difference ($p < 0.005$). This significant difference indicated that the CHX treatment, and not the stationary growth phase, was the major cause of the *rpoE* mutant mortality. In addition, we conducted a gene complementation study. The *rpoE* mutant complemented with the vector pTre99A-*rpoE* was able to completely restore the parental phenotype during the exposure to CHX, clearly showing that the mortality of *rpoE* mutant was due the absence of *rpoE* gene and not to any polar effect caused by the mutation (Figure 1D).

3.2. Effect of the *rpoE* Mutation on the Physiology of *E. coli* O157 during the Early Stationary Growth Phase

In total, 78 protein spots showed significant ($p < 0.05$) shifts in protein abundance between these two organisms due to their

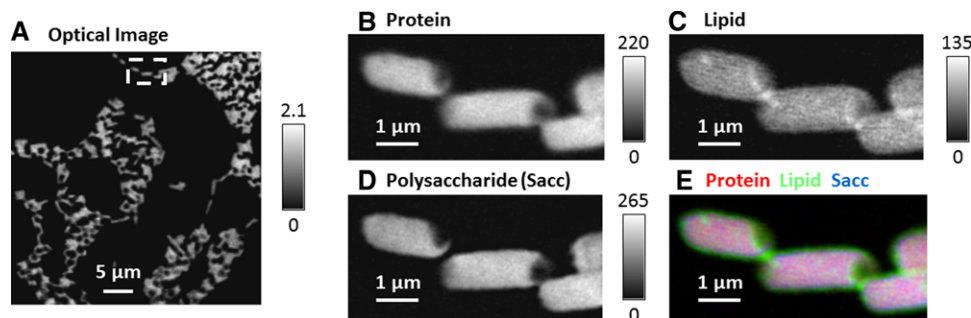


Figure 3. STXM analysis of stationary phase $\Delta rpoE$ *Escherichia coli* O157 mutant control cells (no CHX treatment). A) STXM optical density (OD) image (288.2 eV) of a $30 \times 30 \mu\text{m}$ area. The gray scale indicates optical density. The white rectangle shows the area studied in detail. Component maps of (B) protein, (C) lipid, and (D) polysaccharide. E) Rescaled color-coded composite map of the protein (red), lipid (green), and polysaccharide (blue) component maps.

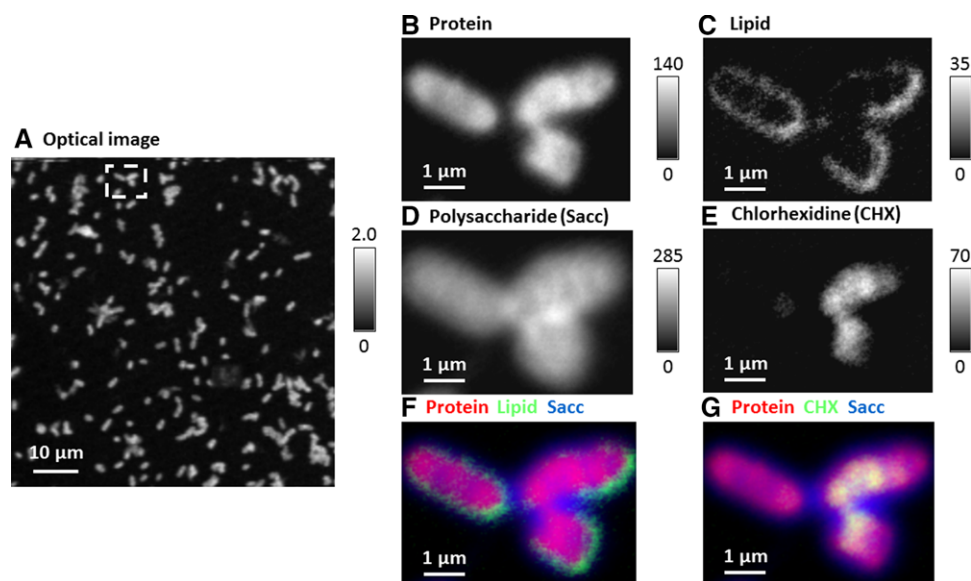


Figure 4. STXM analysis of stationary phase of $\Delta rpoE$ *Escherichia coli* O157 mutant cells treated with $100 \mu\text{g mL}^{-1}$ of CHX for 3 h. A) STXM OD image (288.2 eV) of a $60 \times 60 \mu\text{m}$ area. The gray scale indicates optical density. The white rectangle shows the area studied in detail. Component maps of (B) protein, (C) lipid, (D) polysaccharide, and (E) chlorhexidine. F, G) Rescaled color-coded composite maps of the protein (red), lipid (green), polysaccharide (blue), and chlorhexidine (green) component maps.

(q-PCR): outer membrane protein A (*ompA*), fumarate hydratase class II (*fumC*), dihydrolipoyl dehydrogenase (*lpdA*), hypothetical protein Z1243 (*γcaC*), and elongation factor Ts (*tsf*). The q-PCR analysis, summarized in Supporting Information, Figure 3, indicated a strong correlation ($p = 0.0019$) between the abundances of these proteins and the expression of their genes, with an R^2 value of 0.9728.

3.5. The *rpoE* Mutation Promotes the Intracellular Accumulation of CHX

The component maps of the untreated stationary growth phase $\Delta rpoE$ mutant showed that these cells were surrounded by an outer layer, mainly composed of lipids, while the intracellular milieu was predominantly filled with proteins (Figure 3). In sharp contrast to untreated control cells, the stationary growth phase

$\Delta rpoE$ mutant cells exposed to CHX were found to lack a continuous outer lipid layer, with polysaccharides being the major component now surrounding the cell (Figure 4). This finding indicates that a shift in the composition of the cell envelope occurred following CHX treatment. Furthermore, in comparing the fate of CHX in stationary growth phase wild-type and $\Delta rpoE$ mutant cells, it was observed that the majority of the $\Delta rpoE$ mutant cells (69.2%; 9 out of 13 cells) contained intracellular CHX (Figure 5). In contrast, a smaller fraction of wild-type *E. coli* O157 cells (17.6%; 3 out of 17 cells) contained intracellular CHX. The wild-type cells that did not absorb CHX had a defined LPS outer layer (Supporting Information, Figure 4). Another image portraying the component maps from an image sequence of the wild-type cells treated with CHX revealed that CHX was generally associated with the lipid fraction (Supporting Information, Figure 5), indicating that the lipid layer likely serves a protective role against cationic antimicrobials like CHX.

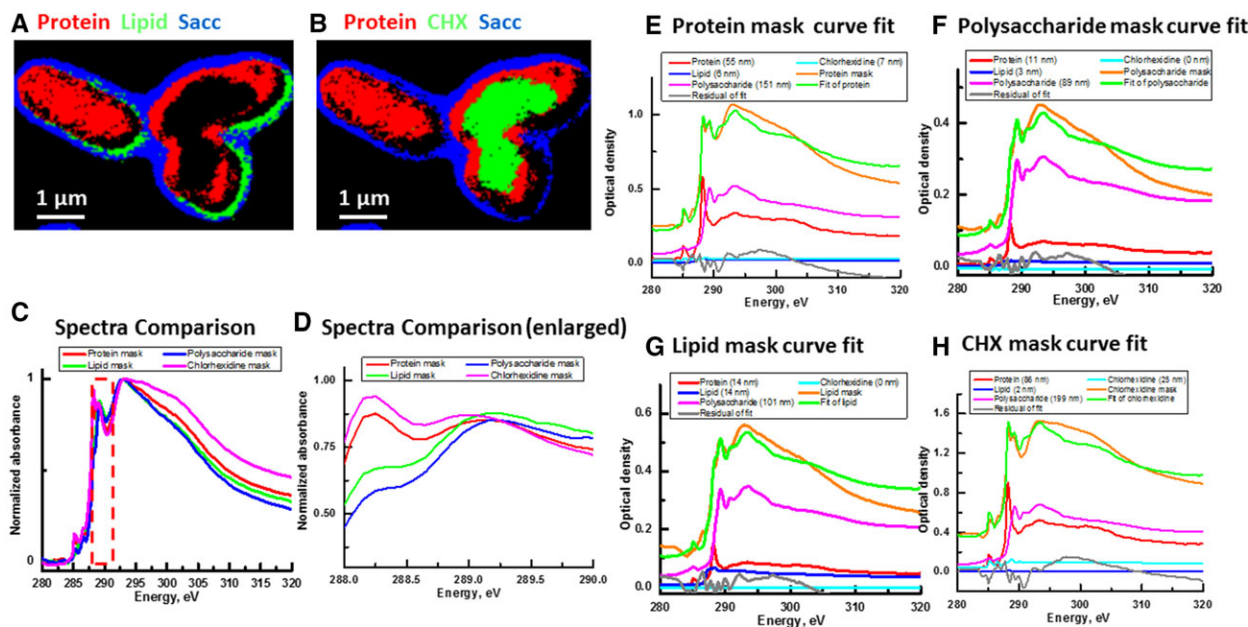


Figure 5. Curve fitting analysis on the STXM spectra derived from the protein, lipid, polysaccharide, and CHX component maps of the stationary phase mutant *Escherichia coli* O157 cells treated with $100 \mu\text{g mL}^{-1}$ CHX. A) Protein (red), lipid (green), and polysaccharide (blue) masks. B) protein (red), CHX (green), and polysaccharide (blue) masks. C) Spectra derived from the areas shown in the masking maps and (D) an enlarged view of the derived spectra over a range of 288–290 eV. Curve fitting of the derived (E) protein (F test = 1130), (F) polysaccharide (F test = 758), (G) lipid (F test = 644) and (H) CHX masks (F test = 848). The values in parenthesis beside the protein, lipid, polysaccharide and CHX in the legend are the thickness in nanometers of the component contributing to the masked spectra.

4. Discussion

The RpoE sigma regulon governs the biogenesis of the bacterial outer membrane and therefore may play a crucial role in protection of Gram-negative bacteria against antimicrobial agents and other stressors that affect the integrity and/or permeability of the outer membrane.^[22] We recently showed that the ESR plays a major role in the protection of *Salmonella enterica* serovar Enteritidis against the bactericidal effect of zinc nanoparticles by mediating the proteolysis of irreversibly-denatured periplasmic proteins, unfolding and refolding periplasmic proteins, trans-envelope trafficking, and cell adhesion.^[7] In the current study, using *E. coli* O157 as a model organism, we found that the *rpoE* mutation conferred growth phase-dependent changes in tolerance to CHX. This growth phase-associated change in tolerance to CHX could be explained by differences in the phenotypic traits and the functionality of the *rpoE* sigma factor between the wild-type and *rpoE* mutant. It has been previously observed in isogenic populations of Gram-negative bacteria that nonreplicating variants (i.e., persister cells) are highly tolerant to antimicrobials, while their rapidly replicating counterparts are susceptible to the same antimicrobial agent.^[23] The *rpoE* mutant is inherently growth deficient (i.e., slow replicating) compared to the parental wild-type. This phenotypic difference between the wild type (i.e., rapidly replicating) and slowly-growing *rpoE* mutant would render the mutant cells less sensitive to CHX during the exponential phase of growth. Upon entry into the early stationary growth phase, both strains would undergo growth arrest and their tolerance to CHX would increasingly become dependent on σ^E

functionality. The resistance of the wild-type and sensitivity of the *rpoE* mutant during the stationary growth phase clearly suggests that the RpoE regulon is of critical importance for cellular homeostasis of this human pathogen during treatment with the antimicrobial, CHX.

To gain insight into the *rpoE*-dependent adaptive response, we carried out a global proteome analysis of mutant and wild-type organisms during the early stationary growth phase at several time points during CHX exposure. Performing gene ontology enrichment cluster analyses, we discovered that the functional group of proteins associated with external encapsulating structures was profoundly altered. This functional group, including outer membrane protein A (*ompA*), outer membrane protein W (*yciD*), outer membrane lipoprotein (*slyB*), glutamate/aspartate periplasmic binding protein (*ybeJ*), and chaperone Skp (*skp*), was downregulated in the wild type compared to that of the *rpoE* mutant strain. To maintain envelope homeostasis during extracytoplasmic stress, σ^E upregulates three small regulatory RNAs, MicA, RybB, and MicL, which antagonize the synthesis of OMPs,^[24–26] thereby reducing the massive flux of membrane proteins toward the envelope. It has previously been shown that the regulatory loop of σ^E has a profound effect on the degree of intrinsic antibiotic resistance in Gram-negative bacteria, as it significantly reduces synthesis and insertion of porin channels and therefore decreases the porin-mediated permeability to antimicrobial agents with small molecules (i.e., beta-lactams, tetracyclines, and chloramphenicols).^[22] Our proteomic data confirmed that the wild-type strain, possessing a functional σ^E , repressed the synthesis of the most abundant outer membrane proteins

in response to the extracytoplasmic stress; whereas, the *rpoE* mutant strain was incapable of employing the same adaptive strategy (see Figure 2B). Here, it is very important to note that CHX, a polycationic agent, penetrates cells of Gram-negative bacteria via a lipid-mediated route and not the porin-mediated pathway,^[22,27] thus decreased porin permeability has no effect on the susceptibility of the Δ rpoE mutant to CHX.

During the CHX treatment time course, the proteomes of the wild-type and the *rpoE* mutant underwent significantly fewer changes compared to the proteomes of these two organisms during the stationary phase prior to CHX treatment. During CHX treatment, the most notable alteration was the upregulation of molecular chaperone proteins, specifically the heat shock proteins IbpA and GroEL, in the proteome of the wild-type strain. GroEL is essential in protein folding of a wide range of nonnative polypeptides, unfolding kinetically-trapped intermediates followed by their proper folding and release. Aside from the upregulation of stress response proteins, alterations in the abundance of enzymes included several key metabolic pathways (i.e., glycolysis, citric acid cycle) in the wild-type proteome. Overall, the relatively mild response of both organisms to CHX treatment may be explained by the fact that the stationary growth phase triggers the expression of σ^E - and σ^S -dependent core genes,^[8,28] which provides cells with the ability to survive stationary phase stress, as well as additional stresses not yet encountered via a phenomenon known as “cross protection.”

To determine whether differences in survival between the *rpoE* mutant and wild-type strains were associated with other structural or functional changes that could influence the binding of polycationic agent CHX to the polyanionic surface of the LPS, an outer leaflet of the outer membrane, high resolution synchrotron-based STXM was undertaken. The STXM data revealed that the majority of mutant cells contained intracellular CHX, while only a small fraction of the wild-type cell population had the same phenotype (i.e., intracellular CHX), revealing that a dysfunctional σ^E leads to the intracellular accumulation of CHX. Analyzing the STXM data, we found that prior to CHX treatment, the *rpoE* mutant had a defined lipid bilayer and that following CHX treatment, the integrity of this bilayer had become compromised, leading to the development of a predominantly “leaky-cell” phenotype in the mutant population. Polycationic agents, such as CHX, bind to the polyanionic surface of the LPS-containing outer leaflet of the outer membrane via electrostatic interactions, perturbing the lipid bilayer and increasing its permeability; this is in accordance with the “self-promoted uptake” hypothesis.^[29] It is important to note that the STXM experiments were conducted using a tenfold higher concentration of CHX than used during the extracytoplasmic stress assay and the comparative proteomic experiments; thus, the effect of perturbation was more pronounced. Irrespective, the STXM data highlights the critical role of the σ^E regulon in maintaining the lipid bilayer during treatment with this antimicrobial agent.

In summary, the final outcome, antimicrobial susceptibility or resistance, appears to be the sum of interactions between σ^E functionality, phenotypic heterogeneity, and bacterial growth conditions. To the best of our knowledge, this is the first report showing that the σ^E regulon is of critical importance in the homeostasis of Gram-negative bacteria exposed to polycationic agents

by virtue of its ability to maintain the integrity of the asymmetric lipid bilayer of the outer membrane.

Abbreviations

CHX, chlorhexidine; ESRs, extracytoplasmic stress responses; OMPs, outer-membrane porins; STXM, scanning transmission X-ray microscopy

Supporting Information

Supporting Information is available from the Wiley Online Library or from the author.

Acknowledgement

The authors gratefully acknowledge the technical support from Daniela Vidovic and Felipe Acosta.

Conflict of Interest

There are no known conflicts of interest associated with this study, or the results, and any of the authors.

Keywords

antimicrobial resistance, extracytoplasmic stress response, outer membrane proteins, *rpoE* sigma factor

Received: July 26, 2017
Revised: November 23, 2017

- [1] World Health Organization. *Antimicrobial Resistance: Global Report on Surveillance*. World Health Organization, Geneva, Switzerland **2014**.
- [2] Centers for Disease Control and Prevention. *Antibiotic Threats in the United States, 2013*. Centers for Disease Control and Prevention, US Department of Health and Human Service, Atlanta, GA **2013**.
- [3] J. Meccas, P. E. Rouviere, J. E. Erickson, T. J. Donohue, C. A. Gross, *Genes Dev.* **1993**, *7*, 2618.
- [4] J. W. Erickson, C. A. Gross, *Genes Dev.* **1989**, *3*, 1462.
- [5] A. De Las Penas, L. Connolly, C. A. Gross, *J. Bacteriol.* **1997**, *179*, 6862.
- [6] T. L. Testerman, A. Vazquez-Torres, Y. Xu, J. Jones-Carson, S. J. Libby, F. C. Fang, *Mol. Microbiol.* **2002**, *43*, 771.
- [7] S. Vidovic, J. Elder, P. Medihala, J. R. Lawrence, B. Predicala, H. Zhang, D. R. Korber, *Antimicrob. Agents Chemother.* **2015**, *59*, 3317.
- [8] G. Rowley, M. Spector, J. Kormanec, M. Roberts, *Nature Rev. Microbiol.* **2006**, *4*, 383.
- [9] M. A. Luzar, T. C. Montie, *Infect. Immun.* **1985**, *50*, 572.
- [10] J. E. Craig, A. Nobbs, N. J. High, *Infect. Immun.* **2002**, *70*, 708.
- [11] S. Lima, M. S. Guo, R. Chaba, C. A. Gross, R. T. Sauer, *Science* **2013**, *340*, 837.
- [12] M. Ehrmann, T. Clausen, *Annu. Rev. Genet.* **2004**, *38*, 709.
- [13] V. A. Rhodius, W. C. Suh, G. Nonaka, J. West, C. A. Gross, *PLoS Biol.* **2006**, *4*, e2.
- [14] S. Vidovic, D. R. Korber, *Appl. Environ. Microbiol.* **2006**, *72*, 4347.
- [15] S. L. K. Choy, Boyle, EC, O. Gal-Mor, D. L. Goode, Y. Valdez, B. A. Vallance, B. B. Finlay, *Infect. Immun.* **2004**, *72*, 5115.

- [16] D. G. Ginzinger, *Exp. Hematology* **2002**, *30*, 503.
- [17] K. V. Kaznatcheev, C. H. Karunakaran, U. D. Lanke, S. G. Urquhart, M. Obst, A. P. Hitchcock, *Proc. 14th Natl. Conf. Synchrotron Radiat. Res. SRI* **2007**, *582*, 96.
- [18] I. N. Koprinarov, A. P. Hitchcock, C. T. McCrory, R. F. Childs, *J. Phys. Chem. B* **2002**, *106*, 5358.
- [19] J. J. Dynes, J. R. Lawrence, D. R. Korber, G. D. W. Swerhone, G. G. Leppard, A. P. Hitchcock, *Sci. Total Environ.* **2006**, *369*, 369.
- [20] Development Core Team. (2011) *R: A Language and Environment for Statistical Computing*. R Foundation for Statistical Computing, Vienna, Austria.
- [21] D. W. Huang, B. T. Sherman, R. A. Lempicki, *Nat. Protoc.* **2009**, *4*, 44.
- [22] H. Nikaido, *Microbiol. Mol. Biol. Rev.* **2003**, *67*, 593.
- [23] T. Dorr, M. Vulic, K. Lewis, *PLoS Genet.* **2009**, *5*, e1000760.
- [24] M. S. Guo, T. B. Updegrave, E. B. Gogol, S. A. Shabalina, C. A. Gross, G. Storz, *Genes Dev.* **2014**, *28*, 1620.
- [25] K. Papenfort, V. Pfeiffer, F. Mika, S. Lucchini, J. C. D. Hinton, J. Vogel, *Mol. Microbiol.* **2006**, *62*, 1674.
- [26] K. I. Udekwu, E. Gerhart, H. Wagner, *Nucl. Acids Res.* **2007**, *35*, 1279.
- [27] H. A. Delcour, *Biochim. Biophys. Acta* **2009**, *1794*, 808.
- [28] H. Weber, T. Polen, J. Heuveling, V. F. Wendisch, R. Hengge, *J. Bacteriol.* **2005**, *187*, 1591.
- [29] M. Vaara *Microbiol. Rev.* **1992**, *56*, 395.